

## **Supplementary Information**

### ***NMNATI* Mutations Cause Leber Congenital Amaurosis**

Marni J. Falk, Qi Zhang, Eiko Nakamaru-Ogiso, Chitra Kannabiran, Zoe Fonseca-Kelly, Christina Chakarova, Isabelle Audo, Donna S. Mackay, Christina Zeitz, Arundhati Dev Borman, Magdalena Staniszewska, Rachna Shukla, Lakshmi Palavalli, Saddek Mohand-Said, Naushin H. Waseem, Subhadra Jalali, Juan C. Perin, Emily Place, Julian Ostrovsky, Rui Xiao, Shomi S. Bhattacharya, Mark Consugar, Andrew R. Webster, José-Alain Sahel, Anthony T. Moore, Eliot L. Berson, Qin Liu, Xiaowu Gai and Eric A. Pierce

Correspondence should be addressed to EAP ([eric\\_pierce@meei.harvard.edu](mailto:eric_pierce@meei.harvard.edu))

## Supplementary Information

### Contents

#### A. Supplementary Note

1. Clinical information for family members of LCA Pedigrees 047, 007, 053
2. Clinical information for family members of LVPEI LCA Pedigrees
3. Clinical information for family members of UCL LCA Pedigrees

#### B. Supplementary Figures

4. *Supplementary Figure 1.* Exome Data Filtering
5. *Supplementary Figure 2.* Pedigrees of additional LCA kindreds with *NMNAT1* mutations
6. *Supplementary Figure 3.* Schematic overview of the role of the *NMNAT1* enzyme in NAD<sup>+</sup> biosynthetic and salvage pathways
7. *Supplementary Figure 4.* *NMNAT1* sequence conservation
8. *Supplementary Figure 5.* Expression and localization of mutant *NMNAT1* protein
9. *Supplementary Figure 6.* Purified, recombinant mutant *NMNAT1* proteins

#### C. Supplementary Table

10. Supplementary Table 1 – *NMNAT1* primers
11. References for Supplementary Information

## A. Supplementary Note

### 1. Clinical information for family members of LCA Pedigrees 047, 007, 053

#### Family 047:

a) **Subject IV-1** is a Pakistani female who had nystagmus onset in the newborn period. Electroretinogram (ERG) performed during early infancy was non-detectable (i.e.  $< 10 \mu\text{V}$ ), leading to a clinical diagnosis of Leber congenital amaurosis (LCA). She showed oculodigital sign since early childhood. Initial ophthalmological evaluation at The Children's Hospital of Philadelphia at age 11 years was significant for nystagmus and enophthalmos. Her anterior segment O.D. was within normal limits and O.S. was significant for a corneal opacity. She was not able to fix on or follow objects. Dilated fundus exam was significant for bilateral optic nerve atrophy, attenuation of the retinal blood vessels, atrophic changes in the macula, and scattered pigment changes in the retinal peripheries in both eyes.

Her additional medical history was significant for severe to profound sensorineural hearing loss that was diagnosed at 2 months of age. A right ear cochlear implant was placed at age 7 years. Her early development was delayed, with her achieving sitting unassisted at age 1 year and walking at age 3. She remains non-verbal. She has been diagnosed with autism and has stereotypical behaviors.

Clinical Genetics evaluation at the Children's Hospital of Philadelphia evaluation at age 11 years was significant for normal stature and weight with relative microcephaly (OFC 5<sup>th</sup> percentile, 50<sup>th</sup> percentile for 5-year-old). Dysmorphic features included low hairline, synophrys, medial eyebrow flare, small forehead, inverted nipples, mild truncal obesity, abdominal protuberance, possible scoliosis, and kyphosis.

Metabolic screening laboratory studies in blood were normal, including comprehensive chemistry panel, quantitative plasma amino acid analysis, blood lactate, blood pyruvate, plasma carnitine, plasma acyl-carnitine profile, very long chain fatty acid analysis, and thyroid hormone screening. Clinical diagnostic sequencing revealed no deleterious mutations in known LCA genes, including *CRB1*, *LRAT*, *TUPL1*, *RPE65*, *AILP1*, *CRX*, *RDH12*, *GUCY2D*, *RPGRIP1*, *CEP290*, *LCA5*, *RD3*, *IMPDH1*, and *SPATA7*. Genome-wide SNP microarray analysis (Illumina HumanQuad610 BeadChip) performed in the CHOP CytoGenomics Laboratory identified several large regions (greater than 10 Mb) of homozygosity, as were consistent with her known consanguinity.

b) **Subject IV-2** is a Pakistani boy who underwent initial Ophthalmology and Clinical Genetics evaluations at The Children's Hospital of Philadelphia at age 8 years. His best corrected visual acuity was 20/30 and he had normal dilated fundus examination. He had a history of strabismus, status-post surgical repair in infancy.

He had bilateral sensorineural hearing loss and wears hearing aids. His early developmental milestones were met at age appropriate ages. However, he had recently been given a clinical diagnosis of Mucopolysaccharidosis Type III based on having clinical features of acquired short stature by age 2 years, progressive elbow and finger contractures, an unprovoked fracture, coarse facies,

and hirsutism. Prior metabolite testing had revealed elevated beta-glucuronidase, beta-galactosidase, alpha-fucosidase and beta-hexosaminidase that were suggestive of a pattern consistent with Mucopolipidosis types II or III. Enzyme activity screening in skin fibroblasts for MPS-I, MPS-II and MPS-VI were reportedly negative. Sequencing of *GNPTAB* was negative. No additional clinical genetic testing was performed.

**c) Subject IV-3** is a Pakistani boy who presented at 1 month of age with no reaction to light and poor visual attention. Ophthalmologic evaluation at age 4 months was significant for myopia, mild pallor of the optic nerves, and vascular attenuation in both retinas. ERG was undetectable for both cone and rod photoreceptor activity in infancy. Brain MRI obtained during early childhood was within normal limits. Initial Ophthalmologic evaluation at The Children's Hospital of Philadelphia at age 3 years, 4 months was significant for light perception only, enophthalmos, normal anterior segments, early atrophy of the optic nerves, attenuation of the retinal blood vessels, as well as atrophy and pigment mottling in the macula and retinal peripheries of both eyes. Follow-up evaluation at The Children's Hospital of Philadelphia at age 4 years was significant for no light perception.

His additional medical history was significant for global developmental delay, with his achieving walking unassisted at age 2 years and he was non-verbal at age 4 years. He had autism spectrum disorder and stereotypical behaviors. He had normal hearing. Clinical Genetics evaluation at age 4 years was significant for relative microcephaly, thick hair, inverted triangular face, enophthalmos, low anterior and lateral hairline with hirsute forehead, synophrys, relative hypertelorism, high arched palate, persistence of the fetal fingertip pads bilaterally, mild 5<sup>th</sup> finger clinodactyly bilaterally, and soft skin.

**d) Additional Kindred Members.** Family members IV-4, IV-5, IV-6, IV-7, and IV-8 reside in Pakistan and were not able to be clinically evaluated by members of this study team. However, medical questionnaires completed by the family provided information about each individual. By report, IV-7 and IV-8 have a similar clinical presentation to IV-1, including congenital blindness, hearing loss, developmental delay, and non-verbal autism. Subject IV-6 has isolated congenital blindness but no developmental delay. Subject IV-4 has isolated congenital hearing loss but no developmental delay.

**Family 007:**

Subject II-2 has a history of reduced vision since early childhood. Ophthalmologic evaluation at The Children's Hospital of Philadelphia at age 3 years was significant for fixing and following and normal anterior segments. Her fundus exam revealed early atrophy of the optic nerves, early attenuation of the retinal blood vessels, and atrophic and pigmentary changes in the retinal peripheries. At this evaluation, her family reported she could recognize colors and preferred bright lights. However, at an annual exam one year later she reported a decline in her visual function and was relying more on tactile sensation, learning Braille, and using a CCTV in the classroom. Visual acuity at age 4 years was significant for light perception only, with an unchanged fundus exam from the prior year. Her medical history was otherwise normal, including normal growth and development. There was no family history of eye disease. Clinical diagnostic sequencing revealed no deleterious mutations in known LCA genes, including *AIPL1*,

*CABP4, CRB1, CRX, GUCY2D, IMPHD1, IQCBI, LCA5, LRAT, OTX2, RD3, RDH12, RPE65, RPGRIP1, SPATA7, and TULP1.*

**Family 053:**

Subject II-1 presented with poor vision and nystagmus in the first few months of life. ERG at age 1 was reportedly “flat” and consistent with the diagnosis of LCA. Ophthalmologic exam at The Children’s Hospital of Philadelphia at age 20 was significant for no light perception. The fundus exam revealed atrophy of the optic nerves and attenuation of retinal blood vessels, atrophy of the retina and choroid in the central maculas, and atrophic changes in the retinal peripheries. Spectralis OCT analysis showed loss of the retinal architecture centrally and thinning of the retina outside of the maculas. His birth history is significant for being born at 33-weeks’ gestational age. He had a history of developmental delay.

**2. Clinical information on family members of LVPEI LCA Pedigrees**

**LVPEI LCA 73:**

Subject II-2 was evaluated at 5 months of age, with visual acuity of fixing on and following light. Retinal examination was significant for the presence of only minimal disc pallor, moderate arterial narrowing, and diffuse RPE degeneration throughout the retina with sparse pigment migration in the retinal peripheries. The macular areas showed atrophic scars of 1.5 disc diameter size. Their condition has remained stable over 3 years of follow-up.

**LVPEI LCA 79:**

Subject IV:1 was evaluated at 1-year-old, with visual acuity of light perception. Retinal examination revealed the presence of moderate disc pallor, moderate arterial narrowing, as well as diffuse and somewhat coarse RPE degeneration throughout the retina with sparse pigment migration in retinal peripheries. In the macular area, there were pigment clumps and RPE degeneration of 2 disc diameters in area around the fovea. The condition has remained stable over 2 years of follow-up. This subject also had a history of motor developmental delay observed at one year of age, for which appropriate physical therapy was started and improvement over the next year was observed.

**LVPEI LCA 100:**

Subject II-2 was evaluated at the age of 3 months, with visual acuity of following and fixing light. Refraction showed hyperopia of + 9.5 D sph with -1.00D cylinder at 180 degrees. Retinal examination showed the presence of only minimal disc pallor, moderate arterial narrowing, as well as diffuse and somewhat coarse RPE degeneration throughout the retina with sparse pigment migration in retinal peripheries. There was a >4 disc diameter area of macular excavation with pigment hypertrophy at the edges and atrophic base. Their condition has remained static at 7 years of follow-up.

**LVPEI LCA 128:**

Subject II-3 was evaluated at 28 years of age. His visual acuity was 20/380 for the right eye and 20/150 for the left eye. Retinal examination showed the presence of only minimal disc pallor, moderate arterial narrowing, as well as diffuse and somewhat coarse RPE degeneration all over

with sparse pigment migration in retinal peripheries. There was a >3 disc diameter area of macular excavation with pigment hypertrophy at the edges and atrophic base in both eyes.

### **3. Clinical information for family members of UCL LCA Pedigrees**

#### **UCL LCA 1:**

Subject II-1 presented to the pediatric ophthalmology clinic at the age of four years. She had poor vision from birth with roving nystagmus and an oculodigital reflex. She was systemically normal. There was no family history of any ocular disease and no evidence of consanguinity. The family are of Caucasian descent. At presentation, her vision in either eye was no perception of light. She had a hypermetropic refractive error at +11.0 diopter sphere in either eye. Ocular examination showed a normal anterior segment. The fundus examination showed bilateral optic disc pallor and severe macular atrophy. There was widespread retinal pigment epithelium atrophy with minimal bone spicule pigmentation in the retinal periphery. ERG revealed an undetectable retinal responses.

#### **UCL LCA 2:**

Subject II-2 had poor vision and nystagmus from birth. She was systemically normal and there was no family history of any ocular disease. The proband had Caribbean and Sri Lankan ancestry. There was no parental consanguinity. When reviewed at age 13 months, the vision in either eye was perception of light. She had a hypermetropic refractive error of +3.0 diopter sphere in each eye. The anterior segments were normal. Fundoscopy showed severe macular atrophy and pigmentation. The retinal vessels were attenuated and there was bilateral pigment epithelial atrophy and retinal pigment deposition. Her ERG showed undetectable retinal responses.

#### **UCL LCA 3:**

Subject II-1 presented with poor vision and nystagmus from birth. She was systemically normal and there was no family history of any ocular disease. The family were from Caribbean descent and there was no parental consanguinity. At the age of 10 years, the corrected vision was 1.5 logMAR in each eye. She had a refractive error of +3.0 diopter sphere in the right eye and +5.0 diopter sphere in the left eye. The anterior segments were normal. Fundus examination revealed severe macular atrophy and pigmentation bilaterally with severe peripheral retinal pigment epithelium atrophy and pigment migration. The retinal blood vessels were attenuated. The ERG was undetectable.

#### **UCL LCA 4:**

Subject II-1 presented with poor vision and nystagmus from birth. He was systemically normal and there was no family history of any ocular disease. He was of mixed race origin with Irish and Caribbean ancestry. At aged 13 months, his vision was perception of light only in either eye and he had a hypermetropic refractive error of +6.5 diopter sphere in either eye. His anterior segments were normal, he had sluggish pupillary responses and fundoscopy showed bilateral severe macular atrophy with peripheral pigment migration. Electroretinography using surface electrodes and non-Ganzfeld stimulation identified a generalised retinal dysfunction affecting the rod and cone photoreceptors, in keeping with a severe photoreceptor dystrophy.

**UCL LCA 5:**

Subject II-2 presented with poor vision from birth with roving nystagmus and an oculodigital reflex. She was systemically and developmentally normal. There was no family history of any ocular disease, but an older sibling was developmentally delayed and had features consistent with an autistic spectrum disorder. This was a non-consanguineous family of Polish descent. At age 18 months, her vision was perception of light in either eye and she had a hypermetropic refractive error of +6.0 diopter sphere in either eye. An adnexal exam showed bilateral enophthalmos and a mild left ptosis. The enophthalmos is likely to have occurred subsequent to her oculodigital reflex. She had normal anterior segments and funduscopy showed severe bilateral macular atrophy with retinal pigment epithelium atrophy and granularity throughout the fundus. The ERG showed undetectable responses.

**UCL LCA 6:**

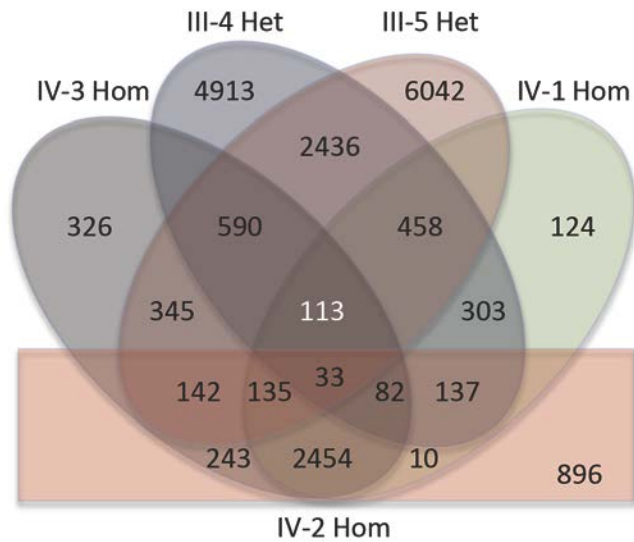
Subject II-1 had poor vision from infancy and was systemically normal. He was diagnosed as having a retinal dystrophy. He was of British Caucasian descent and there was no parental consanguinity. When reviewed at the age of 41 years, his vision was hand movements bilaterally. He had mild nystagmus and bilateral posterior chamber intraocular lens implants *in situ*, reflecting prior cataract extraction surgery. Funduscopy showed extensive bilateral macular atrophy with extensive retinal pigmentation in the periphery.

**UCL LCA 7:**

Subject II-1 presented with poor vision and nystagmus from birth. He was systemically normal and there was no family history of any ocular disease. He was of British Caucasian descent and there was no known consanguinity. At the age of 36 months, his vision was recorded as no perception of light. He had normal anterior segments. Funduscopy showed severe macular atrophy with bilateral optic disc pallor and retinal vessel attenuation. There was widespread retinal pigment epithelium atrophy in the periphery. An ERG performed in infancy showed non-recordable retinal responses.

## B. Supplementary Figures

### 4. Supplementary Figure 1

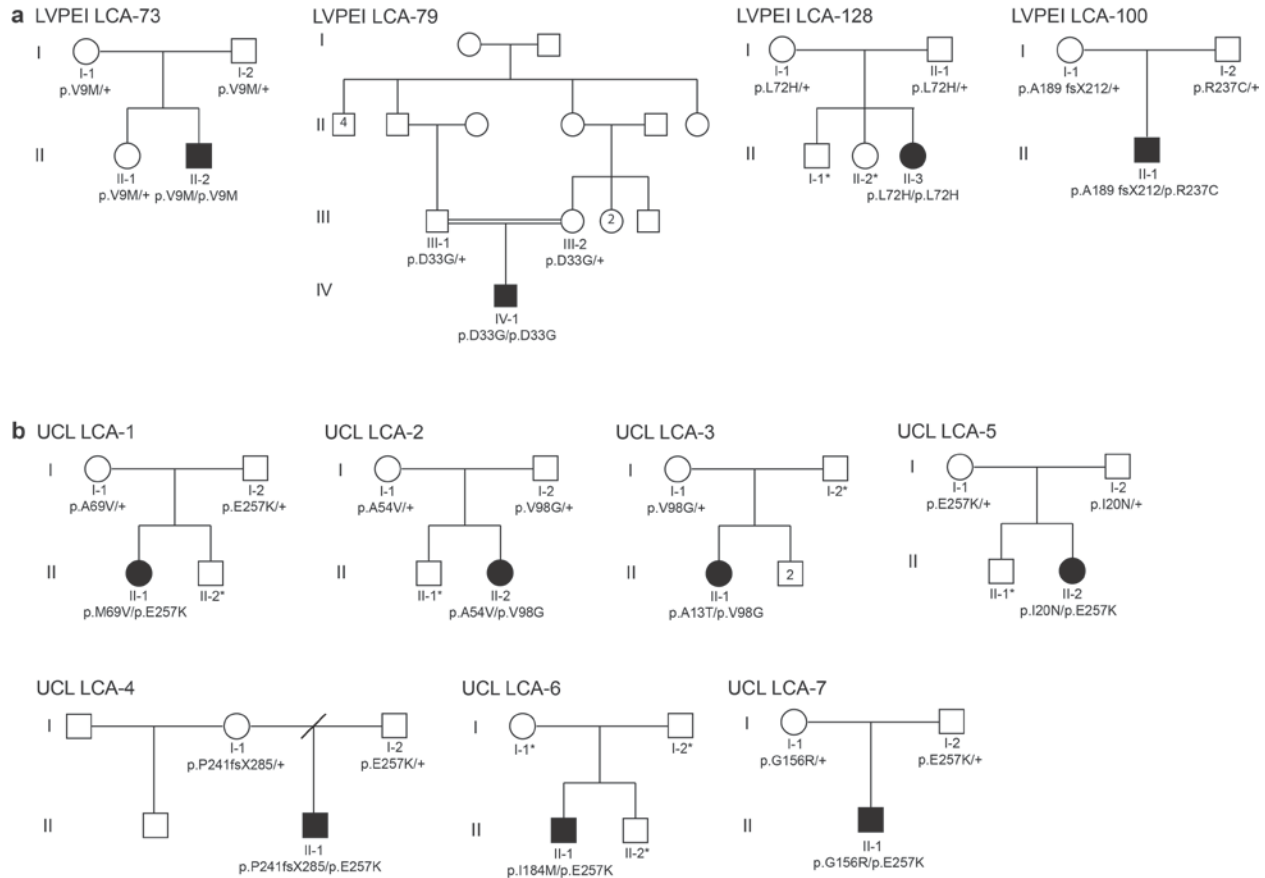


#### ***Supplementary Figure 1. Exome Data Filtering***

Exome sequence data was filtered to identify genes containing non-synonymous homozygous variants present in subjects IV-1 and IV-3 that demonstrated biparental inheritance. Variants that were also found to be homozygous in the visually unaffected sibling (IV-2) were excluded to obtain 113 variants in 86 genes as potentially pathogenic for their LCA phenotype.



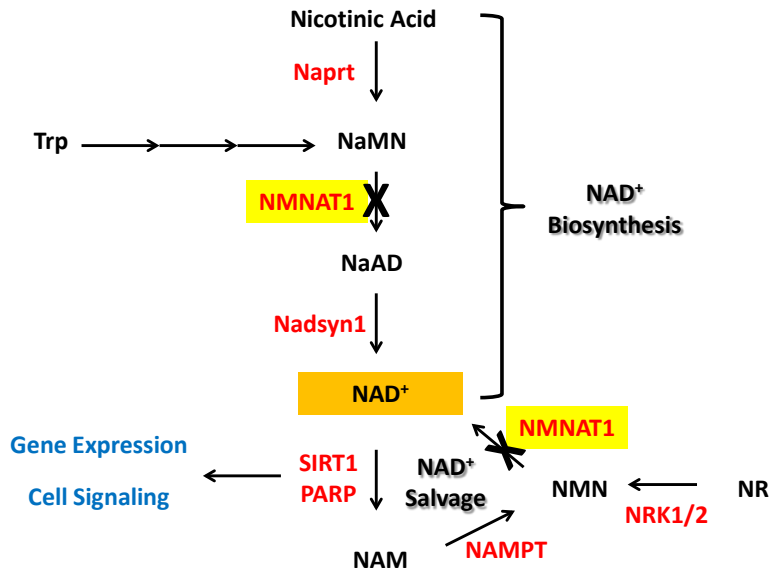
## 5. Supplementary Figure 2



### Supplementary Figure 2. Pedigrees of additional LCA kindreds in which *NMNAT1* mutations were identified.

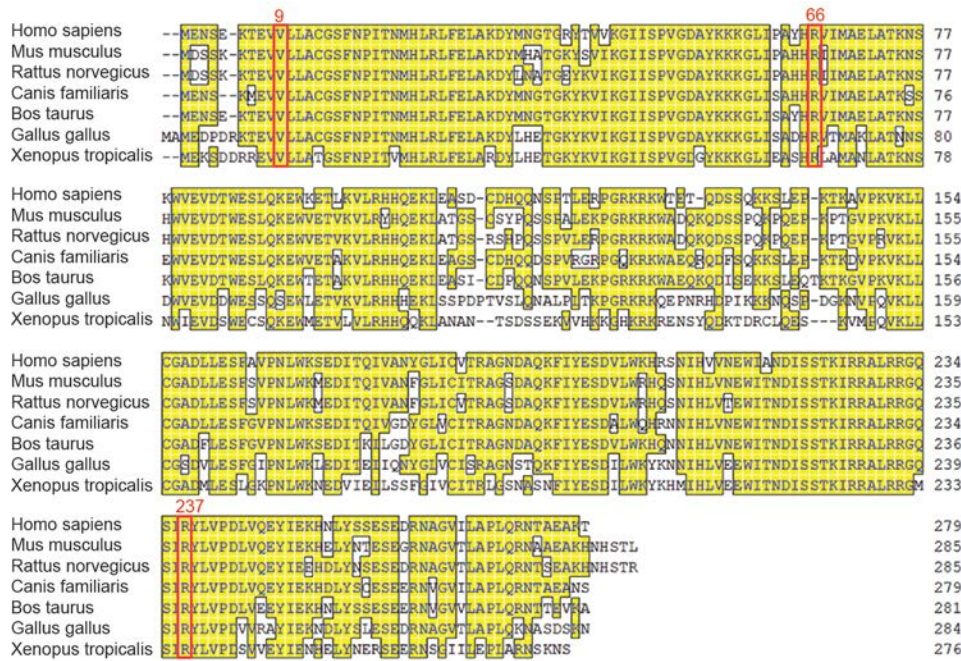
(a) Pedigrees of LCA families from LVPEI with mutations identified in *NMNAT1* by Sanger sequencing. (b) Pedigrees of LCA families from UCL with mutations identified in *NMNAT1* by Sanger sequencing. The identified mutations are indicated. The '+' represents a wild-type allele. Squares and circles indicate male or female, respectively, and numbers within symbols indicate multiple offspring of a given gender. Slashes depict deceased individuals. Individual affected by LCA are indicated by black symbols. \* indicates individuals for which DNA samples are not available. As shown, mutations were detected in an additional individual who was homozygous for the previously identified p.V9M mutation (but apparently unrelated to family 047), as well as in two additional families from LVPEI in which the probands were homozygous for either the c.98A>G (p.D33G) or c.215T>A (p.L72H) mutations, respectively. One LCA family from LVPEI and all 7 LCA families from UCL had compound heterozygous mutations, including one family with the same p.M69V and p.E257K mutations as were identified in CHOP/MEEI family 053.

## 6. Supplementary Figure 3



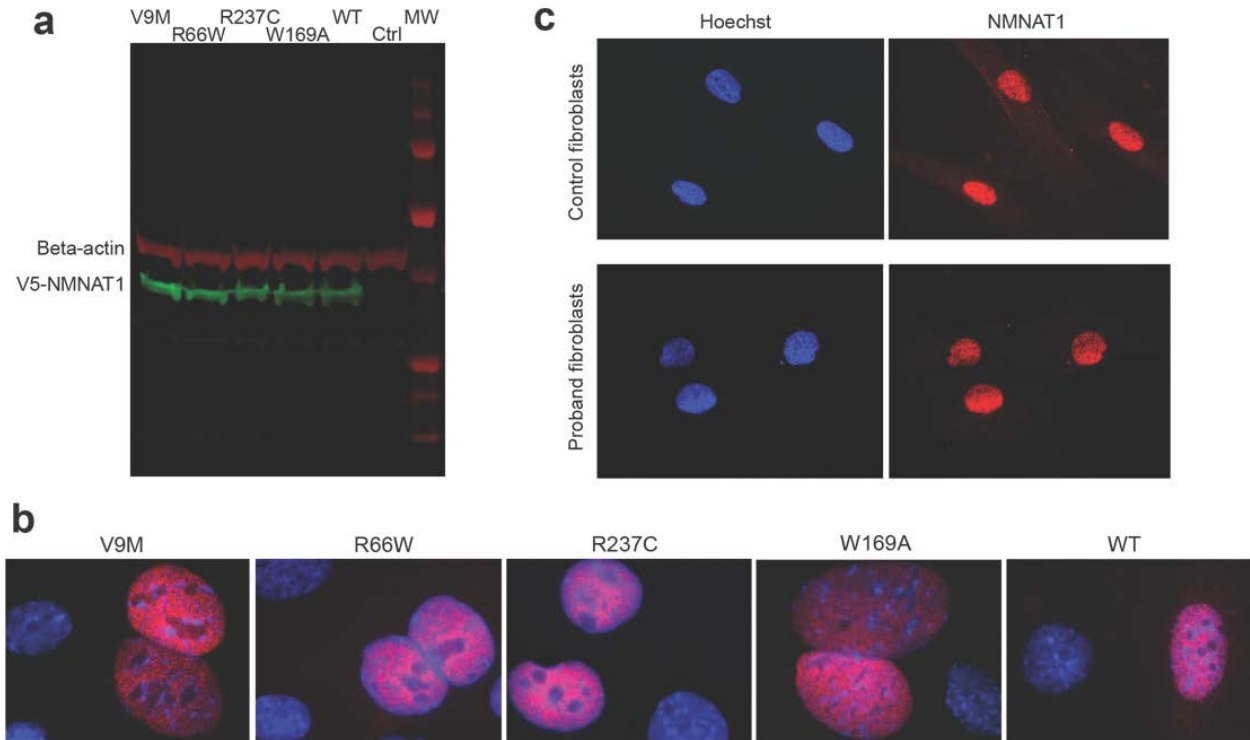
**Supplementary Figure 3. Schematic overview of the role of the NMNAT1 enzyme in NAD<sup>+</sup> biosynthetic and salvage pathways.** The site of the NMNAT1 enzyme deficiency (yellow highlight) caused by a homozygous p.V9M mutation in Penn 047 is indicated by an “X”, which impacts NAD<sup>+</sup> biosynthetic and salvage pathways. NMNAT1, nicotinamide adenyltransferase isoform 1; NAD<sup>+</sup>, nicotinamide adenine dinucleotide; NAM, nicotinamide; NMN, nicotinamide mononucleotide; NR, nicotinamide riboside; NaMN, nicotinic acid mononucleotide; NaAD, nicotinic acid adenine dinucleotide; TRP, tryptophan; Naprt, nicotinic acid phosphoribosyltransferase; Nadsyn1, NAD<sup>+</sup> synthetase; NRK, nicotinamide riboside kinases; NAMPT, nicotinamide phosphoribosyltransferase; SIRT1, sirtuin 1; PARP, poly-ADP-ribose polymerase

## 7. Supplementary Figure 4



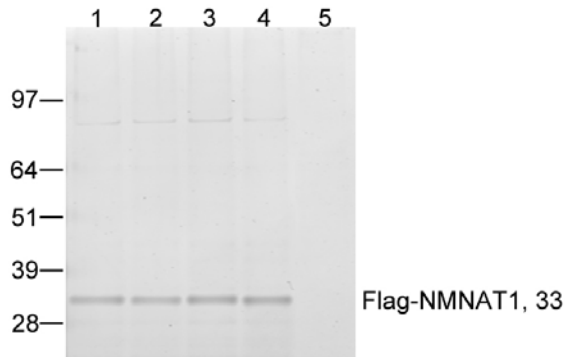
**Supplementary Figure 4. NMNAT1 sequence conservation.** Polypeptide sequences of NMNAT1 from NCBI (human, NP\_073624; mouse, NP\_597679; rat, NP\_001032645; dog, XP\_536739; cow, NP\_001069302; chicken, XP\_417605; Xenopus tropicalis, NP\_001016772) were aligned via Clustal W. Conserved residues are highlighted and boxed. The locations of V9, R66 and R237 are indicated. The crystal structure of the NMNAT1 protein is a barrel-like hexamer, where V9, R66 and R237 are predicted to localize to the outside surface (PDB ID: 1KQN)<sup>1</sup>.

## 8. Supplementary Figure 5



**Supplementary Figure 5.** Expression and localization of mutant NMNAT1 protein. **(a) Recombinant mutant NMNAT1 proteins showed correct expression size and levels in CHO cells.** CHO cells were transfected with plasmids encoding V5-tagged wild-type (WT) NMNAT1, mutant NMNAT1 (p.V9M, p.R66W, or p.R237C mutations identified in LCA families), or a negative control NMNAT1 mutation (p.W169A) having known loss of catalytic activity<sup>2</sup>. Non-transfected cells were also included as a control (Ctrl). Protein extracts harvested from the transfected and control cells were subjected to immunoblotting with anti-V5 antibodies. All five forms of the NMNAT1 protein showed normal size and expression levels. Antibodies to  $\beta$ -actin were used as a gel loading control. **(b) Recombinant mutant NMNAT1 proteins showed correct nuclear localization in the nuclei of transfected mIMCD3 cells.** Mouse IMCD3 cells were transfected with plasmids encoding V5-tagged wild-type (WT), mutant (p.V9M, p.R66W, p.R237C mutations identified in LCA families), or p.W169A (loss of catalytic activity) NMNAT1 proteins. Transfected cells were stained with anti-V5 antibodies (red), and Hoechst dye to demonstrate nuclei (blue). **(c) Endogenous NMNAT1 protein showed correct nuclear localization in the LCA proband's fibroblasts.** Fibroblasts from a normal control and the LCA proband from Family 047 (subject IV-1) were fixed and stained with antibodies to human NMNAT1 (red). The p.V9M mutant NMNAT1 protein localized correctly to the nuclei (Hoechst dye, blue) of the LCA proband's fibroblasts.

## 9. Supplementary Figure 6



**Supplementary Figure 6.** Purified, recombinant mutant NMNAT1 proteins  
Flag-tagged recombinant NMNAT1 proteins were produced and affinity purified as described in Methods. 0.4  $\mu$ g of WT (lane 1), p.Trp169Ala (lane 2), p.Val9Met (lane 3), p.Arg237Cys (lane 4), and p.Arg66Trp (lane 5) proteins were subjected to SDS-PAGE, and the gel stained with Coomassie blue. The wild-type and first three NMNAT1 protein variants are readily detectable, and highly enriched following affinity purification. The p.Arg66Trp protein was not detected. Further experiments will be needed to determine if the Flag-tagged p.Arg66Trp protein is unstable to purification, or if the mutation prevents affinity purification via another mechanism.

## C. Supplementary Table

### 10. Supplementary Table 1 - *NMNATI* primers

Gene	Exon	Annealing Temperature (°C)	Primer Sequence
<i>NMNATI</i>	2	61	F- GGGTGGCAGAGCAAGACCTTATC
			R- ATGCTGGGATTGCAGGTGTG
<i>NMNATI</i>	3	60	F- TGAGCCGAGATCACTCCAGTG
			R- CATCCTTTGGTGCTGTGCTCTAC
<i>NMNATI</i>	4	58	F- TATAGACACCATCAAGAGAAATTGGAGGC
			R- TCAACTCTAGTCCGTGGGTCCTGC
<i>NMNATI</i>	5	60	F- TTTCCACTTGGAGGAGGTAGAGG
			R- ACTCCAGATTGTTTCAGATCCC

### 11. References for Supplementary Information

1. Zhou, T. *et al.* Structure of human nicotinamide/nicotinic acid mononucleotide adenylyltransferase. Basis for the dual substrate specificity and activation of the oncolytic agent tiazofurin. *J Biol Chem* **277**, 13148-54 (2002).
2. Berger, F., Lau, C. & Ziegler, M. Regulation of poly(ADP-ribose) polymerase 1 activity by the phosphorylation state of the nuclear NAD biosynthetic enzyme NMN adenylyl transferase 1. *Proc.Nat.Acad.Sci.* **104**, 3765-70 (2007).